

# Wearable Flexible and Stretchable Glove Biosensor for On-Site Detection of Organophosphorus Chemical Threats

Rupesh K. Mishra,<sup>†,||</sup> Lee J. Hubble,<sup>†,‡,||</sup> Aida Martín,<sup>†,||</sup> Rajan Kumar,<sup>†</sup> Abbas Barfidokht,<sup>†</sup> Jayoung Kim,<sup>†</sup> Mustafa M. Musameh,<sup>§</sup> Ilias L. Kyratzis,<sup>§</sup> and Joseph Wang<sup>\*,†,||</sup>

<sup>†</sup>Department of Nanoengineering, University of California, San Diego, La Jolla, California 92093, United States

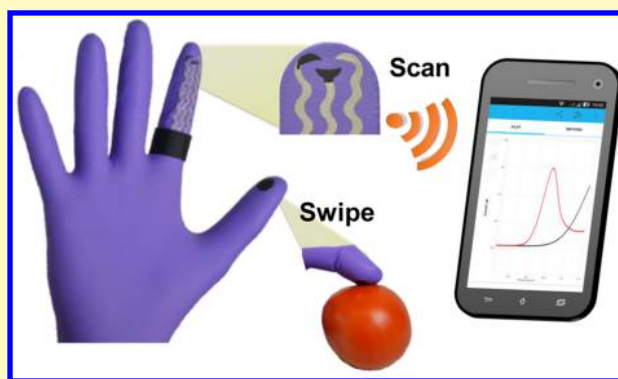
<sup>‡</sup>CSIRO Manufacturing, Lindfield, New South Wales 2070, Australia

<sup>§</sup>CSIRO Manufacturing, Clayton, Victoria 3168, Australia

## Supporting Information

**ABSTRACT:** A flexible glove-based electrochemical biosensor with highly stretchable printed electrode system has been developed as a wearable point-of-use screening tool for defense and food security applications. This disposable-mechanically robust “lab-on-a-glove” integrates a stretchable printable enzyme-based biosensing system and active surface for swipe sampling on different fingers, and is coupled with a compact electronic interface for electrochemical detection and real-time wireless data transmission to a smartphone device. Stress-enduring inks are used to print the electrode system and the long serpentine connections to the wireless electronic interface. Dynamic mechanical deformation, bending, and stretching studies illustrate the resilience and compliance of the printed traces against extreme mechanical deformations expected for such on-glove sampling/sensing operation. An organophosphorus hydrolase (OPH)-based biosensor system on the index finger enables rapid *on-site* detection of organophosphate (OP) nerve-agent compounds on suspicious surfaces and agricultural products following their swipe collection on the thumb finger. The new wireless glove-based biosensor system offers considerable promise for field screening of OP nerve-agents and pesticides in defense and food-safety applications, with significant speed and cost advantages. Such “lab-on-a-glove” demonstration opens the area of flexible wearable sensors to future on-the-hand multiplexed chemical detection in diverse fields.

**KEYWORDS:** wearable sensor, lab-on-a-glove, stretching, chemical warfare agent, organophosphorus hydrolase, mechanical stress, food security



Wearable sensors are uniquely placed to fill the technology gap for real-time analytics at the point-of-need.<sup>1–6</sup> The seamless integration of chemical sensors within wearable platforms gives the power of laboratory-based chemical analyses directly on the wearer's body.<sup>3,5,7–9</sup> Several biosensors, based primarily on enzyme electrodes, have been incorporated recently into cutting-edge wearable devices to allow non-invasive sensing of lactate, glucose, or alcohol in sweat or interstitial fluids,<sup>4,10,11</sup> lactate and uric acid in saliva,<sup>12,13</sup> and glucose in tears.<sup>14,15</sup> While the majority of these wearable sensor systems have focused on fitness and healthcare applications, there are growing demands for developing wearable sensor platforms for monitoring hazardous chemicals for diverse security and environmental applications.<sup>16,17</sup>

This paper introduces a glove-embedded printable biosensor system that withstands extreme mechanical deformations, and used for detecting different organophosphate OP nerve-agent compounds (Figure 1). The increasing use of chemical warfare agents (CWA) represents a major security challenge.<sup>18</sup> In

particular, OP nerve-agents represent a serious concern as they can be weaponized for utility as CWA,<sup>19,20</sup> and are routinely used as pesticides in agricultural and domestic settings.<sup>21,22</sup> These OP neurotoxins severely affect the nervous system and lead to rapid death. Due to the high toxicity of OP nerve-agents and pesticides there are urgent demands for reliable advanced wearable sensor systems for their rapid and selective *on-site* analyses.<sup>17,19,23–25</sup>

The new glove-based biosensor system brings the analysis of OP compounds directly to the user's fingertips. Disposable polymer gloves in combination with screen-printable sensors can provide a scalable, low-cost, and flexible platform to realize wearable point-of-use electrochemical screening tools. “Forensic fingers” for *on-site* voltammetric detection of gunshot residues and explosives<sup>26</sup> and illicit drugs<sup>27</sup> have been described

Received: January 26, 2017

Accepted: March 3, 2017

Published: March 3, 2017



**Figure 1.** Flexible glove biosensor: fabrication, design and performance. (A) Image of the serpentine stencil design employed for printing the glove-based stretchable device. (B) Schematic of (left) the biosensing scan finger (index finger) containing smiling face shape carbon-based counter (CE), working (WE) electrodes and Ag/AgCl-based reference electrode (RE), and (right) collecting thumb finger with its printed carbon pad; scale bar 10 mm. (C) Photographs of the biosensing index finger under 0% (left) and 50% (right) linear stretch; scale bar, 10 mm. (D) On-glove swiping protocol for sampling chemical threat residues from tomato and stainless steel surfaces. (E) On-glove sensing procedure by joining the index (scan) and thumb (collector) fingers to complete the electrochemical cell. (F, G) Photographs of the wearable glove biosensor, consisting of a sensing finger, containing the immobilized OPH enzyme layer, and the collector/sampling finger. The electrodes are connected via an adjustable ring bandage to the portable potentiostat (attached to the back of hand) for on-site detection with wireless communication to a smartphone for rapid presentation of the voltammetric results. (Inset) Schematic of the interface between potentiostat and glove sensor. The connections consist of a (iii) velcro fabric containing (ii) the aluminum-tape based pins that are adjusted as a ring with the glove sensing connectors and (i) the wiring with the potentiostat.

recently. No glove-based biosensing operations have been demonstrated to date, and no attention has been given to the mechanical resilience of such a wearable sensing system.

Glove-based sensors are required to comply with the extreme and dynamic mechanical deformations associated with their sampling and sensing operation. To impart the high resilience against extreme mechanical deformations expected during the glove sampling/sensing operation we relied here on the combination of stress-enduring inks and serpentine microstructures. The new glove biosensor platform thus utilizes printed serpentine patterns,<sup>28,29</sup> with two levels of stretchability due to the intrinsic stretchability of tailored-made printable inks and the unwinding of the serpentine structure (Figure 1A–C). Careful attention has thus been given to the elastomeric, electrical, and electrochemical properties of the new inks and the printed patterns for withstanding large strain deformations. Dynamic mechanical deformation, bending, and stretching studies have demonstrated the high resilience against extreme mechanical deformations expected in real-life applications of the new chemical-agent biosensing glove. Such compliance with

the complex glove surface is achieved while retaining the attractive electrical and electrochemical properties of the printed electrodes.

Unlike early fingertip voltammetric assays of explosives and illicit drugs,<sup>26,27</sup> the present study represents the first example of performing fingertip enzymatic assays. Such glove-based biocatalytic measurements require carrying out the swipe sampling and electrochemical biosensing steps on different fingers, with the enzyme immobilized on the index finger and the thumb finger used for collecting the nerve-agent residues (Figure 1). The enzyme organophosphorus hydrolase (OPH) has been widely used for electrochemical and optical measurements of OP compounds.<sup>23,24,30,31</sup> As illustrated in Figure 1D and E, fingertip sampling of OP threat residues from the target surface onto the thumb “collector” is followed by joining this finger with the sensing (index) finger for completing the “electrochemical cell”. A carbon disk printed at the thumb tip ensures adhesion of the analyte residues to the collection surface while a conductive semisolid gel matrix (covering the enzymatic OPH/Nafion layer) offers completion of the

electrochemical cell. Finally, the electrochemical detection is carried out using a wireless-based portable miniaturized potentiostat, attached on the back of the hand and connected using a ring bandage for easy reusability, as shown in Figure 1F. G. Scanning-potential square-wave voltammetry (SWV) is used for detecting the *p*-nitrophenol product of the biocatalytic OPH hydrolysis reaction to offer an additional dimension of selectivity compared to common fixed-potential OPH amperometric biosensors. The voltammetric results are transmitted wirelessly for rapid presentation on a mobile device (e.g., smartphone). The “on-hand” detection of different OP chemical agents on a variety of surfaces and agricultural foodstuffs demonstrate that the new wireless glove biosensor holds considerable promise for real-time *on-site* screening of chemical threats for meeting the demands of different military, forensic, consumer protection, and food safety applications.

## EXPERIMENTAL SECTION

**Chemical and Reagents.** Purple nitrile powder-free exam gloves (Kimberly-Clark, Roswell, GA), carbon ink (E3449, Ercon, Inc., Wareham, MA) and Ag/AgCl ink (E2414, Ercon, Inc., MA), platinum-catalyzed silicone elastomer Ecoflex 00-30 (Smooth-On, Inc., Macungie, PA), and permanent fabric adhesive (Aleene's, Inc., Fresno, CA) were used. Potassium ferricyanide, xylene, dipotassium hydrogen phosphate ( $K_2HPO_4$ ), potassium dihydrogen phosphate ( $KH_2PO_4$ ), sodium acetate, polystyrene-*block*-polyisoprene-*block*-polystyrene (PS-PI-PS) (styrene 14 wt %), methyl paraoxon, methyl parathion, Nafion, and ethanol were purchased from Sigma-Aldrich. All chemicals were of analytical grade and were used without further purification. Ultrapure deionized water was used in the preparation of the aqueous electrolyte solutions. Gelatin, fruits, and vegetables were purchased from the local shops of San Diego, CA. The OPH enzyme (10  $\mu\text{g}/\text{mL}$ ) was isolated from *E. coli* bacterial strain DHS $\alpha$ . The isolation, expression, purification, and crystallization were performed following the procedure described by Yang et al.<sup>32</sup> and provided by CSIRO, Australia. The OPH enzyme stability in Nafion was evaluated for several days with a stable electrochemical response observed for up to 3 days, after which the response decreases gradually.

**Preparation of Stretchable Carbon and Ag/AgCl Inks and Electrode Fabrication.** Intrinsically stretchable carbon ink was prepared by mixing Ercon carbon ink (8.3156 g) with PS-PI-PS prepared in xylene (0.4440 g, 5.07 wt %). The beads of PS-PI-PS (1 g) were dissolved in xylene (8 mL), mixed thoroughly in an ultrasonic bath, and then homogenized in a shaker for 2 h. Thereafter, the carbon/PS-PI-PS composite ink was suitable for screen-printing. The PS-PI-PS was used for its hyperelastic properties as a binder in the development of stress-enduring inks.<sup>33</sup> The intrinsically stretchable Ag/AgCl ink was prepared by thoroughly mixing Ercon Ag/AgCl ink (9.5174 g) with Ecoflex (1.443 g, 13.16 wt %) using a SpeedMixer (DAC 150.1 FVZ, FlackTek, Inc., Landrum, SC) for 5 min (2500 rpm). Ecoflex 00-30 was prepared in-house by mixing equal volumes of prepolymer A with prepolymer B provided by the supplier.

The fabrication process utilized a semiautomatic MPM-SPM screen printer (Speedline Technologies, Franklin, MA). The long serpentine interconnected with working area (smiley face shape of 12.14 mm<sup>2</sup> area were designed using AutoCAD (Autodesk, San Rafael, CA) and outsourced for fabrication on stainless steel through-hole 12"  $\times$  12" framed stencils of 125  $\mu\text{m}$  thickness (Metal Etch Services, San Marcos, CA). The planar finger molds (10.0  $\times$  2.3  $\times$  1.3 cm<sup>3</sup> dimensions) were designed using SolidWorks 3D CAD (DS SolidWorks, Waltham, MA) and printed using a Mojo 3D printer (Stratasys, Eden Prairie, MN). The 3D printed molds were inserted into the purple nitrile gloves, to facilitate a planar printing surface, immediately before screen-printing the serpentine structures. The printing process on the sensing (index) finger comprised of a 125  $\mu\text{m}$  thick layer sequence of (a) Ag/AgCl (E2414, Ercon, Inc., Wareham, MA) mixed with Ecoflex, (b) Ercon carbon ink mixed with PS-PI-PS, and (c) an insulating layer comprised of flexible, stretchable adhesive (Aleene's, Inc., Fresno, CA). The Ag/

AgCl-based ink served for the reference electrode, and all serpentine contacts, while the carbon inks were used for printing the working and counter electrodes. The insulating layer was carefully printed on the serpentine interconnects to provide a dielectric separation of the three electrode system and avoids device short-circuits. On the collection (thumb) finger, a circular carbon pad disk (1 cm diameter) was printed using Ercon carbon ink mixed with PS-PI-PS. The screen-printed stretchable electrode patterns were cured at 75  $^\circ\text{C}$  for 10 min after each layer was printed.

### Immobilization of OPH Enzyme on the Working Electrode.

Prior to OPH enzyme immobilization, the working electrode surface was cleaned by applying cyclic voltammetry (CV) in the range 0 to +1.0 V using 0.01 M sodium acetate buffer (pH 4.6) with a scan rate of 0.1 V/s for 20 cycles. Following this, the bioreagent layer was fabricated by coating the working electrode with a mixed Nafion/OPH layer. This was achieved by first preparing a solution of 1% Nafion in ethanol, and a separate solution of OPH (10  $\mu\text{g}/\text{mL}$ ) in 0.1 M phosphate buffer (pH 7.4). The Nafion and OPH solutions were then mixed (500  $\mu\text{L}$ ) at a 7:3 v/v ratio and a 5  $\mu\text{L}$  aliquot of this mixture was drop-casted onto the clean working electrode surface (on the index finger). The electrode was left to dry at room temperature for at least 2 h.

**Electrochemical Studies.** Electrochemical characterization was performed at room temperature using a PalmSens hand-held potentiostat (EmStat3 Blue with 10.0  $\times$  6.0  $\times$  3.4 cm<sup>3</sup> dimensions, PalmSens, Houten, Netherlands) powered by a rechargeable Li–Po battery. The data were transmitted to a smartphone through wireless communications, while using a smartphone app to perform the measurements. To study the effect of applied strain on electrochemical behavior, CV was performed using 2 mM potassium ferricyanide in 1 M KCl over the voltage range  $-0.6$  to  $+0.6$  V with a scan rate of 0.1 V/s. The OP sensing studies were performed by completing the “electrochemical cell” by joining the collection (thumb) finger with the sensing (index) finger (covered with 2.5 wt % gelatin gel) (Figure 1E) and recording the signal of the *p*-nitrophenol product by SWV over the range between +0.4 and +1.2 V using SWV waveform parameters of 10 Hz frequency, 25 mV amplitude and 4 mV potential increment with a quiet time of 5 s.

**Mechanical Resiliency Studies.** The effect of mechanical stress on the printed stretchable gloves was analyzed by electrochemical measurements, optical micrographs and dynamic study of the resistance of Ag/AgCl and carbon-based serpentine structures printed on the glove. The stretching tests were conducted on a custom stretching stage consisting of a motorized linear stage and controller (A-LST0250A-E01 Stepper Motor and Controller, Zaber Technologies, Vancouver, Canada). The samples were programmed to constantly stretch at a speed of 0.6 mm s<sup>-1</sup> from 0% to 50% and back to 0% as one cycle, which takes approximately 70 s; see Video S1. Bending experiments were carried out by completely bending the fingers to 180 $^\circ$  and returning to a normal straight position, as shown in Video S2 for 60 complete cycles (straight-bend-straight). CV studies were carried out before and after 60 iterative stretching and bending steps. Resistance studies were carried out by dynamic testing using an Agilent 34411A digital multimeter (Agilent Technologies, Inc., Santa Clara, CA), sampling at a frequency of 1 Hz, and the Keysight BenchVue software (Keysight Technologies, Inc., Santa Rosa, CA) as a measuring interface. Optical micrographs were taken using a Nikon Eclipse 80i, 4 $\times$  objective illuminated with a Nikon MKII fiber optics light. The images were acquired at 10 frames/s with a Photometrics CoolSnap HQ2 1392  $\times$  1040 pixels CCD camera attached to the microscope and were processed with Metamorph 7.7.5 software (Molecular Devices, Sunnyvale, CA).

### OP Swiping and Scanning on Various Surfaces and Foods.

The various target surfaces and foods were first rinsed with absolute ethanol, then distilled water and dried. Subsequently, the surfaces were contaminated using two OP compounds methyl paraoxon and methyl parathion (200  $\mu\text{M}$  each in 5% v/v acetonitrile). A 200  $\mu\text{L}$  aliquot of each OP compound was cast on the surface of the fruits and vegetables (apples, grapes, green peppers, and tomatoes) and other target surfaces, such as wood, stainless steel, plastic, and glass; the aliquot was



allowed to dry to a residue through evaporation at room temperature for 3–4 h. The printed glove sensor was worn for the sampling and detection steps. Swiping of these surfaces with the thumb finger was accomplished by abrasively rubbing them to mechanically “collect” analyte residues onto the printed carbon disk. A conductive semisolid gel matrix was used to complete the “electrochemical cell” by slightly modifying the protocol described by De Wael et al.<sup>27</sup> In brief, a mixture of 2.5 wt % gelatin in a 100 mM KCl and 100 mM KH<sub>2</sub>PO<sub>4</sub> buffer was heated in a small glass vial at 100 °C for 15 min (600 rpm, until homogenized). The solution was then loaded into a 5 mL syringe in which the hydrogel was formed and aged for a few hours at room temperature before use. The used hydrogel displayed high stability over 2 weeks. Four drops of the gel (200  $\mu$ L) were added to the index finger, surrounded by an O-ring (12.5 mm diameter  $\times$  1.8 mm thickness, that keeps the gel in place) and fixed to the finger using super glue. The thumb (with the collected analyte residues) was brought in contact with the index finger (containing conductive gel) to achieve a complete electrical circuit essential for performing the electrochemical (SWV) measurements. Each glove was used for one-time analysis carried out in the fume-hood for safety.

## RESULTS AND DISCUSSION

**Glove Design and Concept.** The wearable glove biosensor was fabricated using large-scale low-cost screen-printing technology. Figure 1A shows the “lab-on-a-glove” concept, fabrication and methodology for OP screening on various surfaces. The stencil is positioned on top of the purple nitrile glove surface inserted with a planar 3D printed mold, then a rubber squeegee is displaced, dragging the stress-enduring inks and filling the designed hole patterns of the stencil. The fabrication of this glove biosensor requires two glove fingers, the index finger, termed as the “sensing finger” containing the three-electrode biosensor (Figure 1B, left) and the thumb, termed as the “collection finger” used for sampling the threat residues (Figure 1B, right). The sensing finger is based on three different layers of elastic inks printed on the nitrile glove surface. First, a silver layer based on Ag/AgCl particles combined with the elastomeric Ecoflex material, shown to withstand high degrees of strain and stretchability.<sup>34</sup> This layer is used both as the reference electrode and the serpentine connections along the finger down to the third knuckle, where an adjustable ring bandage allows the connection between the glove and the hand-held miniaturized potentiostat (see Figure 1F,G). The second flexible layer consists of a carbon ink, modified with an elastomeric styrene-isoprene copolymer that imparts intrinsic stretchability,<sup>35</sup> which is used to form the working and counter electrodes. Finally, the third and top layer is a transparent flexible stretchable insulator, which covers of the serpentine connections while exposing the sensing area and square contact pads. The two printed elastic layers on the sensing finger are capable of increasing the stretchability features of the sensor without compromising the electrical and electrochemical properties. This offers a 50% stretchability (Figure 1C) to withstand mechanical strains associated with the wearer’s actions and sensing operation. The serpentine structure of the interconnects allows an extended level of stretchability by design, to compliment the intrinsic material stretchability associated with the formulation of the new stress-enduring inks. On the contrary, the collection thumb finger is based on single printed trace, consisting of 1 cm diameter circular pad of a stretchable carbon ink to withstand the mechanical stress during the swiping/sampling of OP residues on different surfaces.

The new stretchable glove biosensor offers rapid, *on-site* sampling and detection of nerve-agent threats on a variety of

surfaces. The on-glove assay consists of two steps, the “swipe” (collection) and “scan” (detection). Figure 1D illustrates the sampling of OP residues from a tomato skin (left) and from a stainless steel surface (right), representative of food safety and general security applications, respectively. The second “scan” step, shown in Figure 1E, is the electrochemical sensing, carried out by joining the index (sensing) and thumb (collector) fingers. A conductive semisolid gel on the sensing area of the index finger provides a medium for analyte diffusion from the collection pad toward the OPH enzyme layer on the working electrode, as well as the conductivity essential for completing the electrochemical cell. Finally, the electrochemical detection of the *p*-nitrophenol (an OP hydrolysis product) is recorded by SWV using a wearable electrochemical analyzer (shown in Figure 1G). The connections to the square contact pads are made using an adjustable ring bandage for easy reusability and interuser adjustment (Figure 1F and G). The resulting voltammetric response is wirelessly transmitted to a smart-phone via the built-in wireless communication feature of the hand-held analyzer.

**Mechanical deformation studies.** The combined use of stress-enduring inks and serpentine microstructures provides the resilience necessary for accommodating large strain deformations experienced during the on-glove sensing operation. To study the effect of different mechanical deformations occurred on a glove, the electrochemical properties of the printed sensor were investigated first using cyclic voltammetry (CV) of the ferricyanide redox probe. The first set of experiments were designed to study the effect of repetitive bending of the glove fingers (Figure 2A) and stretching of the nitrile glove (Figure 2B) upon the CV behavior (Figure 2A,i and 2B,i, respectively). The bending experiments were carried out by completely bending the three joints of the sensing finger and returning to a straighten position, as shown in Video S1 and pictures in Figure 2A,iii. The CV was first measured for a nonbended glove sensor (Figure 2A,i (black plot)), followed by a CV recorded after the 60 bending cycles (red plot). Comparison of the ferricyanide CVs recorded before (Figure 2A,i (black plot)) and after these cycling (Figure 2A,i (red plot)) showed that both the redox potentials and the peak current heights of the redox probe remain similar, even after applying different strains on the electrodes and electrical contacts. These CVs indicate that the bending deformation had a negligible effect on the electrochemical properties of the printed glove. Figure 2A,ii shows the optical micrograph of the printed silver serpentine trace before and after the bending stress. The printing process results in well-defined Ag/AgCl serpentine traces, with a characteristic rough surface, on the glove sensing finger. No significant visual changes of these traces are observed in one of the most affected surfaces during the bending experiments. Thus, both electrochemical behavior and optical images indicate the attractive stress-enduring capabilities afforded by the designed serpentine interconnects and the intrinsically stretchable inks used for device fabrication.

Similar CV experiments were carried out for evaluating the influence of the glove stretching upon the ferricyanide redox behavior. Figure 2B,i displays CV recorded before applying any deformation to the glove surface (black plot) and after 60 repeated 50% stretching cycles of the sensing-finger, and subsequently returning to the initial position (red plot). This repeated stretching strain has a negligible effect upon the CV current and potential characteristics. In contrast, optical micrographs of the serpentine interconnects (Figure 2B,ii)

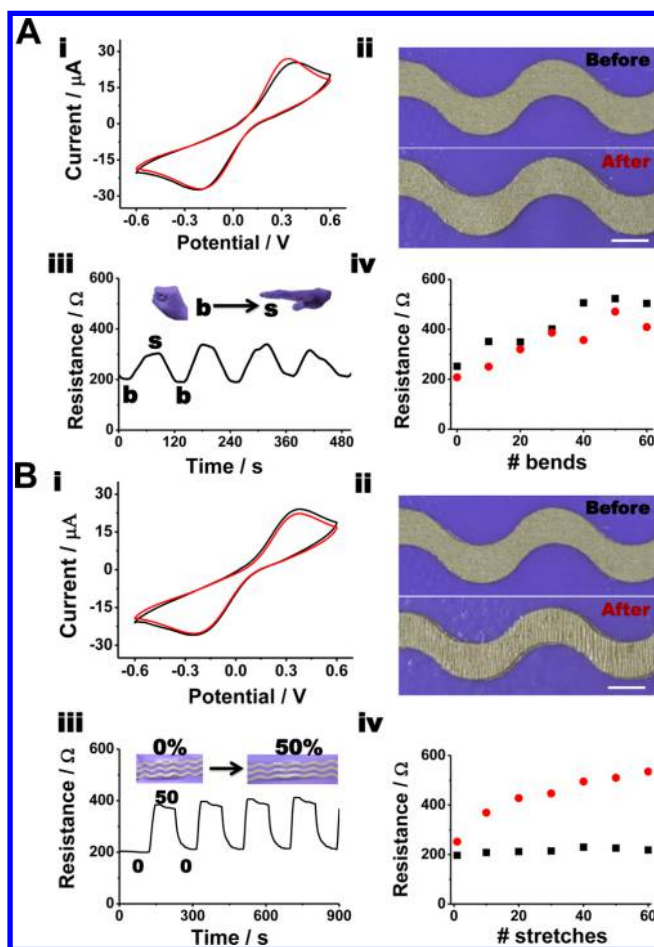


**Figure 2.** Influence of extreme strain levels. Influence of (A) bending and (B) stretching stress upon the electrical and structure characteristics. (i) Cyclic voltammetry of 2 mM ferricyanide in 0.1 M KCl recorded before (black plot) and after (red plot) applying 60 iterative (A) bend and straight finger movements and (B) from 0 to 50% stretching cycles. (ii) Photographs of the serpentine structures (Ag/AgCl Ercon ink/Ecoflex) before (top) and after (bottom) (A) 60 continuous bending of the sensing finger and (B) 60 stretching cycling up to 50% and 100%; scale bars, 2 mm. Dynamic resistance study from the working to the end of the silver contact pad (iii) during four consecutive iterations (A) from complete bending of the fingers (b) to a straight level (s) for 1 min each, (inset) photograph of on-hand movement and (B) from 0% to 50% stretching degree (inset) photograph of studied stretching levels. (iv) Resistance data point for 60 consecutive deformations of the glove for complete bend (red dots) to straight (black square) positions of the fingers (as in A) and from 0% (black square) to 50% (red dots) stretching of the sensing finger (as in B).

after such 60 stretching cycles indicate visible cracks perpendicular to the applied force. However, as indicated from the CVs (Figure 2B,i), such cracks has a negligible effect upon the electrochemical behavior, as supported by the minimal resistance changes discussed below.

Afterward, we examined the influence of such extreme strain levels upon the resistance of the printed traces. A study of the dynamic resistance change was carried out upon repeated bend/straight and stretch/relax cycling of the glove fingers shown in Videos S1 and S2, respectively. Figures 2A,iii,iv and S1A illustrate the dynamic resistance data during these continuous strain cycles. The resistance was measured between the carbon-based working electrode to the end of the silver

contact pads, from a complete bending of the glove fingers to a fully straight level (indicated with the letters b and s, respectively) using 1 min time intervals between movement and cycling. The first 20 cycles (Figure S1A) show resistance values around  $329 \pm 38 \Omega$  for the straight position of the fingers, and  $246 \pm 48 \Omega$  for the complete bended position. The lower resistance value obtained at the bended position versus the nonbended position is attributed to the higher compression applied to the material at the bended position, as shown in the micrographs (Figure S1B). Even after 100 bending cycles, the resistance values are 416 and 430  $\Omega$  for the bended and straight positions, respectively, indicating that numerous repeated bending of the glove has only a mild effect on the electrode resistance that does not compromise the performance of the glove-based biosensor. Figures 2B,iii, iv and S1C show the corresponding dynamic resistance changes during repeated stretch and relax cycles. Study of the 50% stretching shows no significant change of the resistance values at the relax position (0%),  $210 \pm 6 \Omega$ , during the initial 20 stretching cycles (see Figure S1C). However, at a 50% stretch, the resistance increases and nearly plateaus around 500  $\Omega$  after 60 stretching cycles (Figure 2B,iv). Further studies were carried out using 100% stretching indicated an average resistance value of 480  $\Omega$  at the relax stage with an 8% change after 30–60 cycles (see Figure S2). Overall, these glove stretching tests demonstrated minimal resistance changes after intense mechanical stress. These changes are not expected to affect the results of the electrochemical biosensing procedure. It should be noted that these mechanical deformation experiments were carried out at strain and stretch levels that greatly exceed those expected during the glove sensing operation.

**On-Glove Nerve-Agent Sensing.** In this wearable glove biosensor, the OPH is immobilized on the working electrode of the sensing index finger by drop casting with Nafion polymeric film. During the sampling of OP residues, the collection finger, containing the printed carbon disk, swiped the tested surface, as was shown earlier in Figure 1D. The presence of OPs was detected by joining sensing and collection fingers, as was previously discussed in Figure 1E. The OPH/Nafion layer of the sensing finger was covered with conducting gelatin gel (200  $\mu\text{L}$  of 2.5 wt %) to complete the electrochemical cell and also to provide a stable electrolyte. Consequently, a stable and smooth baseline was obtained without any background noise.

In order to test the potential of the glove biosensor for OP detection on various common surfaces, blind sampling and screening studies relevant to defense and food security are presented in Figures 3 and 4, respectively. The sampling in Figure 3A shows photographs of the glove swiping on various target surfaces, including glass (i), wood (ii), stainless steel (iii), and plastic (iv). Three blind tests were carried out for each of the four surfaces. Two different OP chemical agents, methyl parathion (MP) and methyl paraoxon (MPOx), were used to contaminate the surfaces at 200  $\mu\text{M}$  concentrations, with a third test (control) involving an OP-free, noncontaminated surface. Sensing of the enzymatically liberated OP hydrolysis product was carried out by SWV owing to its distinct sensitivity and speed advantages. Figure 3B illustrates the resulting response following swiping these different MP-contaminated surfaces. A well-defined SWVs response, characteristic of the *p*-nitrophenol oxidation peak is observed at +0.85 V indicating the success of the sampling and the sensing. It is worth noting that this glove sensor is designed for a single-use, hence sample cross-contamination is eliminated. As can be seen from the SWVs,

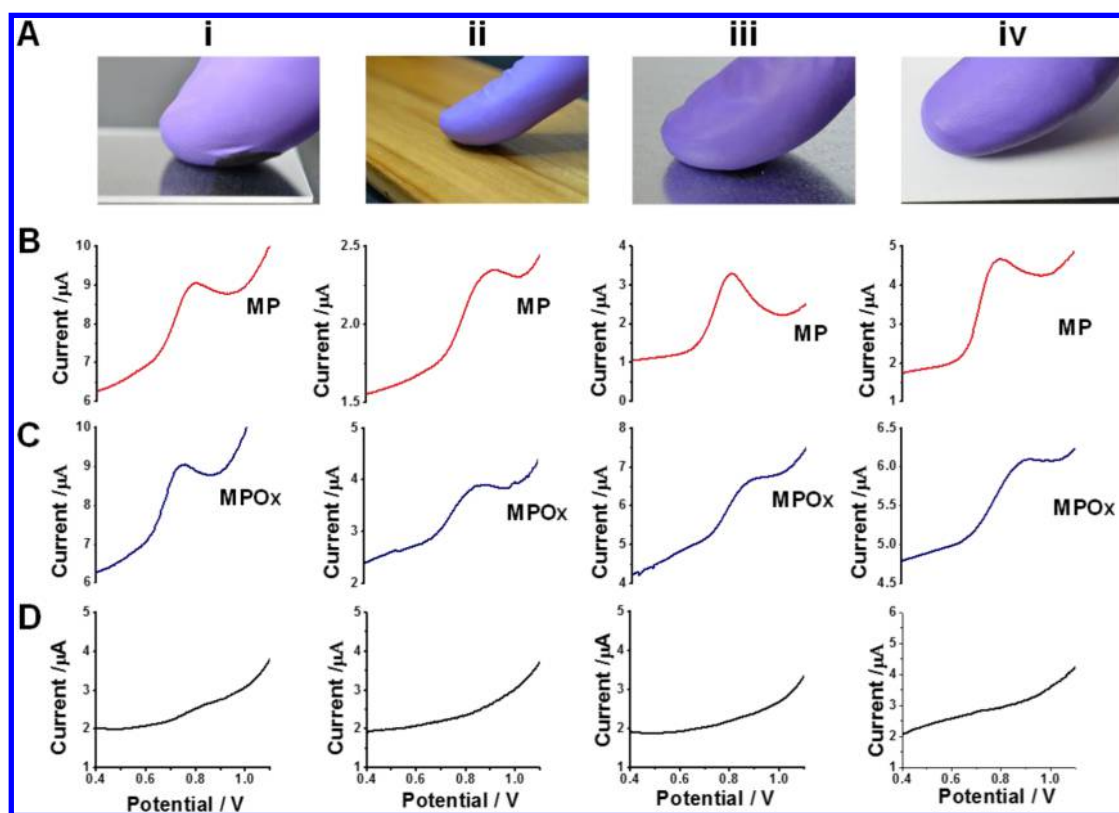


**Figure 3.** Sampling and on-site glove-based screening of OP chemical agents: Toward defense security monitoring. (A) Photographs during sampling on contaminated surfaces of (i) glass, (ii) wood, (iii) stainless steel, and (iv) plastic. SWVs screening of blind samples contaminated with (B) MP, (C) MPOx, along with (D) control OP-free surfaces shown in (A). SWV conditions: voltage range, +0.30 to +1.20 V vs Ag/AgCl; amplitude, 25 mV; and frequency, 10 Hz.

some variability in the peak height is observed between glove tests on different surfaces depends. This reflects various factors such as swiping consistency, surface characteristics, joining of the index and thumb fingers, and diffusion of the analytes within the conductive gel. Such variation has not effect on the qualitative OP detection, corresponding to presumptive screening goal of the new OPH-glove sensor (as indicated from the control experiments for OP-free surfaces described below). These swipe/sensing surface assays were conducted in triplicate for both MPOx and MP pesticides and exhibited good analytical characteristic with relative standard deviations (RSD) of 3.5% and 2.77% ( $n = 12$  gloves) for MPOx and MP, respectively, in terms of redox potential. While our main goal is to obtain qualitative alert for the presence of nerve agents, such peak variations allow semiquantitative information regarding the level of these agents on the target surface. Figure 3C shows similar screening detection for MPOx, showing clear detectable peaks for the *p*-nitrophenol hydrolysis product at +0.85 V. Finally, Figure 3D displays analogous swipe/sense SWV measurements for the four OP-free surfaces. As expected from the absence of OP residues, no *p*-nitrophenol is observed in these four control experiments. Similarly, no SWV anodic response was observed in control experiments using OP contaminated surfaces but without the immobilized OPH. (Figure S3C, D). The absence of the *p*-nitrophenol peak in these control experiments confirmed the importance of the enzyme for the glove-based OP biosensing.

The presence of OP pesticide residues in agricultural products threatens both human and animal health and is thus of significant public concern.<sup>36</sup> Swipe sampling has been used

for the collection of trace residues from agricultural products in connection to mass spectroscopy analysis of food shipments in border points of entry. Such agriculture and food security concerns have inspired us to evaluate the glove OPH biosensor for screening different fruits and vegetables on which OP traces are possibly present. Figure 4A shows photographs of the thumb (collector) finger swiping the skin surface of apple (i), tomato (ii), grape (iii), and green pepper (iv). Following the strategy used earlier for defense security monitoring, three blind tests were carried out for each of the four fruit samples. Two different OP compounds, MP and MPOx were used to contaminate the surfaces (using 200  $\mu$ M concentration solutions) along with a third (control) test carried out on an OP-free noncontaminated surface. Figure 4B demonstrates a clear screening detection of MP for the four different food items (fruits and vegetables). The well-defined SWV peak of the *p*-nitrophenol product at +0.85 V indicates a successful on-glove sampling/sensing procedure and reflects relatively improved interglove reproducibility with %RSD of 3.05 and 2.10 ( $n = 12$  gloves) for MPOx and MP, respectively, compared with the data obtained for the surfaces in Figure 3.<sup>37,38</sup> Similarly, well-defined *p*-nitrophenol signals are observed in Figure 4C for glove-based swiping and biosensing of the pesticide MPOx on these agricultural products. In contrast, no response is observed in the control experiments (Figure 4D) involving the same fruit surfaces but without the pesticide contamination. Similarly, no SWV anodic response was observed in control experiments using OP contaminated surfaces but without the immobilized OPH (Figure S3A, B). Overall, the data within Figure 4 clearly demonstrate the power



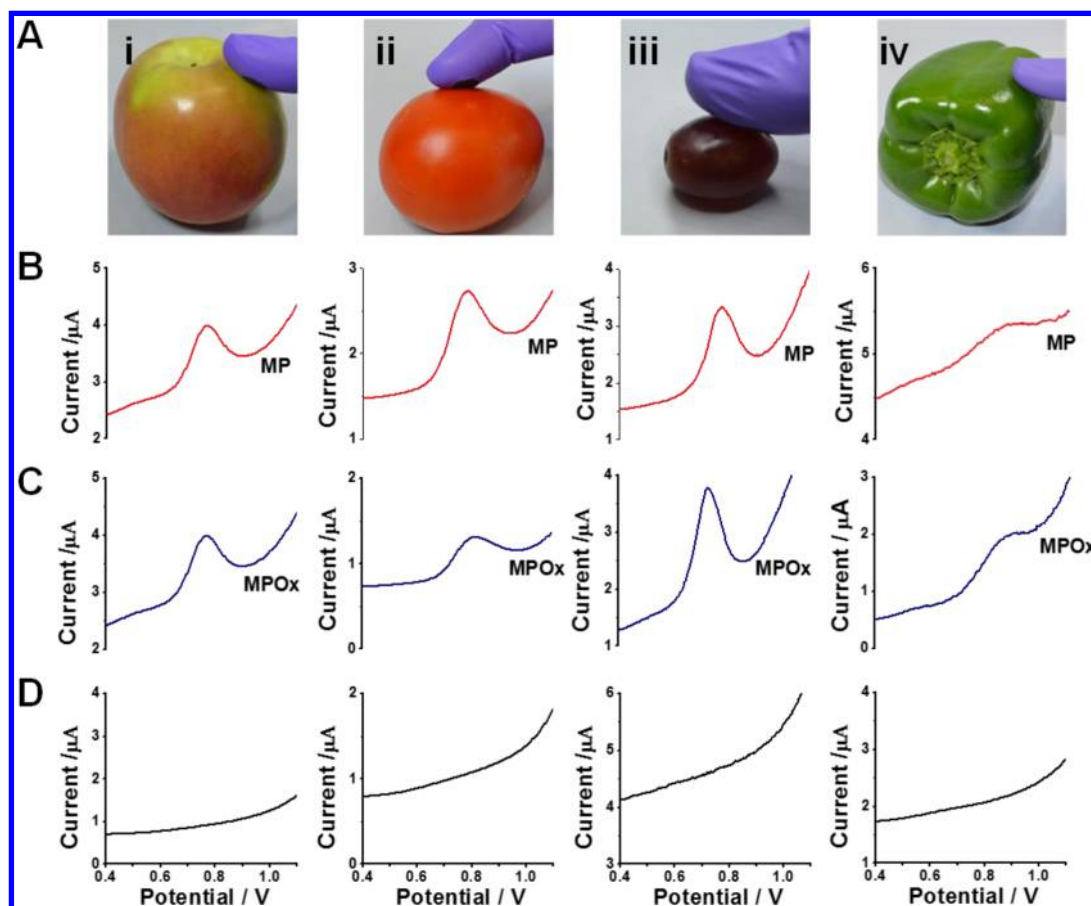


**Figure 4.** Sampling and detecting OP pesticides on the surfaces of different fruits and vegetables: Toward food security monitoring. (A) Photographs during sampling on (i) apple, (ii) tomato, (iii) grape, and (iv) green pepper contaminated surfaces. SWVs for screening of blind samples contaminated with (B) MP, (C) MPOx, along with (D) control food surfaces without the OP contamination. SWV conditions, as in Figure 3.

of the glove biosensor method for rapid *on-site* screening for pesticide-contaminated agricultural products, and for food quality and safety control, in general.

## CONCLUSIONS

We reported on the development of glove-embedded printable biosensors that withstand extreme mechanical deformations, and demonstrated its potential for *on-site* field detection of different OP nerve-agent compounds. The new flexible, wearable “lab-on-a-glove” integrates an enzyme-immobilized biosensing detection finger, the sampling finger, along with real-time wireless data transmission to a smartphone device. Excellent resiliency against mechanical deformations has been achieved by coupling stress-enduring ink materials with printable serpentine-patterned interconnects to the sensing fingers to offer seamless integration with the dynamic glove surface. The new glove-based OPH biosensor addresses the challenges associated with reliable and rapid field screening and detection of chemical threats. It also offers considerable promise toward *on-site* food safety and security applications. Future efforts are aimed at further miniaturization of the electronic backbone through a custom-designed ring-based electronic device and expanding the scope of glove biosensors to the fingertip analysis of a variety of other target compounds. The new generation of flexible glove-based chemical sensors thus represents a logical extension of the scope of wearable devices toward a wide range of safety, security, and forensic applications in variety of field settings.

## ASSOCIATED CONTENT

### Supporting Information

The Supporting Information is available free of charge on the ACS Publications website at DOI: [10.1021/acssensors.7b00051](https://doi.org/10.1021/acssensors.7b00051).

Mechanical studies including, resistance data of bending and stretching and on-glove nerve-agent sensing controls (PDF)

Stretching of the glove sensor, five iterative stretches at 50% and 100% stretch (AVI)

Bending of the glove sensor, dynamic resistance study during total of 100 bends (AVI)

## AUTHOR INFORMATION

### Corresponding Author

\*E-mail: [josephwang@ucsd.edu](mailto:josephwang@ucsd.edu).

### ORCID

Joseph Wang: 0000-0002-4921-9674

### Author Contributions

||R.K.M, L.J.H, and A.M contributed equally to this work.

### Notes

The authors declare no competing financial interest.

## ACKNOWLEDGMENTS

This work was supported by the Defense Threat Reduction Agency Joint Science and Technology Office for Chemical and

Biological Defense (HDTRA 1-16-1-0013). L.J.H. acknowledges travel support partially provided by the “John Philip Award for the Promotion of Excellence in Young Scientists” by CSIRO. The authors thank Dr. Yuan Gao and Dr. Colin Scott (CSIRO) for their help in purifying the OpdA enzyme.

## REFERENCES

- (1) Bandodkar, A. J.; Jeerapan, I.; Wang, J. Wearable Chemical Sensors: Present Challenges and Future Prospects. *ACS Sens.* **2016**, *1*, 464–482.
- (2) Gao, W.; Emaminejad, S.; Nyein, H. Y. Y.; Challa, S.; Chen, K.; Peck, A.; Fahad, H. M.; Ota, H.; Shiraki, H.; Kiriya, D.; et al. Fully integrated wearable sensor arrays for multiplexed in situ perspiration analysis. *Nature* **2016**, *529*, 509–514.
- (3) Rogers, J. A.; Someya, T.; Huang, Y. Materials and Mechanics for Stretchable Electronics. *Science* **2010**, *327*, 1603–1607.
- (4) Jia, W.; Bandodkar, A. J.; Valdés-Ramírez, G.; Windmiller, J. R.; Yang, Z.; Ramírez, J.; Chan, G.; Wang, J. Electrochemical tattoo biosensors for real-time noninvasive lactate monitoring in human perspiration. *Anal. Chem.* **2013**, *85*, 6553–6560.
- (5) Heikenfeld, J. Bioanalytical devices: Technological leap for sweat sensing. *Nature* **2016**, *529*, 475–476.
- (6) Koh, A.; Kang, D.; Xue, Y.; Lee, S.; Pielak, R. M.; Kim, J.; Hwang, T.; Min, S.; Banks, A.; Bastien, P.; et al. A soft, wearable microfluidic device for the capture, storage, and colorimetric sensing of sweat. *Sci. Transl. Med.* **2016**, *8*, 366ra165.
- (7) Zuliani, C.; Diamond, D. Opportunities and challenges of using ion-selective electrodes in environmental monitoring and wearable sensors. *Electrochim. Acta* **2012**, *84*, 29–34.
- (8) Modali, A.; Vanjari, S. R. K.; Dendukuri, D. Wearable Woven Electrochemical Biosensor Patch for Non-invasive Diagnostics. *Electroanalysis* **2016**, *28*, 1276–1282.
- (9) Bandodkar, A. J.; Jia, W.; Wang, J. Tattoo-Based Wearable Electrochemical Devices: A Review. *Electroanalysis* **2015**, *27*, 562–572.
- (10) Bandodkar, A. J.; Jia, W.; Yardımcı, C.; Wang, X.; Ramirez, J.; Wang, J. Tattoo-based noninvasive glucose monitoring: a proof-of-concept study. *Anal. Chem.* **2015**, *87*, 394–398.
- (11) Kim, J.; Jeerapan, I.; Imani, S.; Cho, T. N.; Bandodkar, A.; Cinti, S.; Mercier, P. P.; Wang, J. Noninvasive Alcohol Monitoring Using a Wearable Tattoo-Based Iontophoretic-Biosensing System. *ACS Sens.* **2016**, *1*, 1011–1019.
- (12) Kim, J.; Imani, S.; de Araujo, W. R.; Warchall, J.; Valdés-Ramírez, G.; Paixão, T. R.; Mercier, P. P.; Wang, J. Wearable salivary uric acid mouthguard biosensor with integrated wireless electronics. *Biosens. Bioelectron.* **2015**, *74*, 1061–1068.
- (13) Kim, J.; Valdes-Ramirez, G.; Bandodkar, A. J.; Jia, W.; Martinez, A. G.; Ramirez, J.; Mercier, P.; Wang, J. Non-invasive mouthguard biosensor for continuous salivary monitoring of metabolites. *Analyst* **2014**, *139*, 1632–1636.
- (14) Yao, H.; Liao, Y.; Lingley, A. R.; Afanasiev, A.; Lähdesmäki, I.; Otis, B. P.; Parviz, B. A. A contact lens with integrated telecommunication circuit and sensors for wireless and continuous tear glucose monitoring. *J. Micromech. Microeng.* **2012**, *22*, 075007.
- (15) Pankratov, D.; González-Arribas, E.; Blum, Z.; Shleev, S. Tear based Bioelectronics. *Electroanalysis* **2016**, *28*, 1250–1266.
- (16) Malzahn, K.; Windmiller, J. R.; Valdés-Ramírez, G.; Schöning, M. J.; Wang, J. Wearable electrochemical sensors for in situ analysis in marine environments. *Analyst* **2011**, *136*, 2912–2917.
- (17) Zhu, R.; Azzarelli, J. M.; Swager, T. M. Wireless Hazard Badges to Detect Nerve-Agent Simulants. *Angew. Chem.* **2016**, *128*, 9814–9818.
- (18) Noort, D.; Benschop, H. P.; Black, R. M. Biomonitoring of exposure to chemical warfare agents: a review. *Toxicol. Appl. Pharmacol.* **2002**, *184*, 116–126.
- (19) Kingery, A. F.; Allen, H. E. The environmental fate of organophosphorus nerve agents: a review. *Toxicol. Environ. Chem.* **1995**, *47*, 155–184.
- (20) Bajgar, J. Organophosphates Nerve Agent Poisoning: Mechanism of Action, Diagnosis, Prophylaxis, and Treatment. *Adv. Clin. Chem.* **2004**, *38*, 151–216.
- (21) Gupta, R. C.; Milatovic, D. Toxicity of organophosphates and carbamates. In *Mammalian Toxicology of Insecticides*, Marrs, T., Ed.; Royal Society of Chemistry: Cambridge, UK, 2012, p 104.
- (22) Sharma, D.; Nagpal, A.; Pakade, Y. B.; Katnoria, J. K. Analytical methods for estimation of organophosphorus pesticide residues in fruits and vegetables: A review. *Talanta* **2010**, *82*, 1077–1089.
- (23) Zhang, W.; Asiri, A. M.; Liu, D.; Du, D.; Lin, Y. Nanomaterial-based biosensors for environmental and biological monitoring of organophosphorus pesticides and nerve agents. *TrAC, Trends Anal. Chem.* **2014**, *54*, 1–10.
- (24) Singh, V. V. Recent Advances in Electrochemical Sensors for Detecting Weapons of Mass Destruction. A Review. *Electroanalysis* **2016**, *28*, 920–935.
- (25) Wang, J.; Krause, R.; Block, K.; Musameh, M.; Mulchandani, A.; Schöning, M. J. Flow injection amperometric detection of OP nerve agents based on an organophosphorus-hydrolase biosensor detector. *Biosens. Bioelectron.* **2003**, *18*, 255–260.
- (26) Bandodkar, A. J.; O'Mahony, A. M.; Ramírez, J.; Samek, I. A.; Anderson, S. M.; Windmiller, J. R.; Wang, J. Solid-state Forensic Finger sensor for integrated sampling and detection of gunshot residue and explosives: towards 'Lab-on-a-finger'. *Analyst* **2013**, *138*, 5288–5295.
- (27) de Jong, M.; Slegers, N.; Kim, J.; Van Durme, F.; Samyn, N.; Wang, J.; De Wael, K. Electrochemical fingerprint of street samples for fast on-site screening of cocaine in seized drug powders. *Chem. Sci.* **2016**, *7*, 2364–2370.
- (28) Bandodkar, A. J.; Jeerapan, I.; You, J.-M.; Nuñez-Flores, R.; Wang, J. Highly Stretchable Fully-Printed CNT-based Electrochemical Sensors and Biofuel Cells: Combining Intrinsic and Design-induced Stretchability. *Nano Lett.* **2016**, *16*, 721–727.
- (29) Jeerapan, I.; Sempionatto, J. R.; Pavinatto, A.; You, J.-M.; Wang, J. Stretchable Biofuel Cells as Wearable Textile-based Self-Powered Sensors. *J. Mater. Chem. A* **2016**, *4*, 18342–18353.
- (30) Burnworth, M.; Rowan, S. J.; Weder, C. Fluorescent sensors for the detection of chemical warfare agents. *Chem. - Eur. J.* **2007**, *13*, 7828–7836.
- (31) Mulchandani, A.; Pan, S.; Chen, W. Fiber-optic enzyme biosensor for direct determination of organophosphate nerve agents. *Biotechnol. Prog.* **1999**, *15*, 130–134.
- (32) Yang, H.; Carr, P. D.; McLoughlin, S. Y.; Liu, J.-W.; Horne, I.; Qiu, X.; Jeffries, C.; Russell, R.; Oakeshott, J. G.; Ollis, D. Evolution of an organophosphate-degrading enzyme: a comparison of natural and directed evolution. *Protein Eng., Des. Sel.* **2003**, *16*, 135–145.
- (33) Kumar, R.; Shin, J.; Yin, L.; You, J. M.; Meng, Y. S.; Wang, J. All-Printed, Stretchable Zn-Ag<sub>2</sub>O Rechargeable Battery via, Hyperelastic Binder for Self-Powering Wearable Electronics. *Adv. Energy Mater.* **2016**, 1602096.
- (34) Cánovas, R.; Parrilla, M.; Mercier, P.; Andrade, F. J.; Wang, J. Balloon-Embedded Sensors Withstanding Extreme Multiaxial Stretching and Global Bending Mechanical Stress: Towards Environmental and Security Monitoring. *Adv. Mater. Technol.* **2016**, *1*, 1600061.
- (35) Bandodkar, A. J.; López, C. S.; Vinu Mohan, A. M.; Yin, L.; Kumar, R.; Wang, J. All-printed magnetically self-healing electrochemical devices. *Sci. Adv.* **2016**, *2*, e1601465.
- (36) Lehotay, S. J.; Kok, A. d.; Hiemstra, M.; Bodegraven, P. v. Validation of a fast and easy method for the determination of residues from 229 pesticides in fruits and vegetables using gas and liquid chromatography and mass spectrometric detection. *J. AOAC Int.* **2005**, *88*, 595–614.
- (37) Verkouteren, J.; Coleman, J.; Fletcher, R.; Smith, W.; Klouda, G.; Gillen, G. A method to determine collection efficiency of particles by swipe sampling. *Meas. Sci. Technol.* **2008**, *19*, 115101.
- (38) Crawford, E.; Musselman, B. Evaluating a direct swabbing method for screening pesticides on fruit and vegetable surfaces using direct analysis in real time (DART) coupled to an Exactive benchtop



orbitrap mass spectrometer. *Anal. Bioanal. Chem.* **2012**, *403*, 2807–2812.